P7.139. THE WRF LIGHTNING FORECAST ALGORITHM: RECENT UPDATES AND RESULTS FROM CONVECTIVE ENSEMBLE FORECASTS

Eugene W. McCaul, Jr.[1],Jonathan L. Case[2], Scott R. Dembek[1],
Fanyou Kong[3], Steven J. Goodman[4], and Steven J. Weiss[5]
1. Universities Space Research Association, Huntsville, AL
2. ENSCO and NASA SPoRT, Huntsville, AL
3. Center for Analysis and Prediction of Storms, University of Oklahoma
4. NOAA/NESDIS, Silver Spring, MD
5. NOAA/SPC, Norman, OK

1. INTRODUCTION

Three years ago, McCaul et al. (2009) devised and published a simple, empirical proxy-based method for converting selected fields from convection-allowing models (Kain et al. 2010) into horizontal two-dimensional fields of estimated lightning flash origin density. Since then, interest from the forecasting community has led to its incorporation into a number of explicit-convection forecast models, allowing more widespread testing and analysis of its performance across varying seasons and locations. To date, the Lightning Forecast Algorithm (LFA) of McCaul et al. (2009) has been incorporated in the Weather Research and Forecasting (WRF; Skamarock et al. 2008) model runs performed daily at the National Severe Storms Laboratory (NSSL), the WRF ensembles run each Spring by the Center for Analysis and Prediction of Storms (CAPS) at the University of Oklahoma, and, more recently, in the High Resolution Rapid Refresh (HRRR) runs disseminated by the National Oceanic and Atmospheric Administration (NOAA) Environmental Science Research Laboratory (ESRL). Results compiled from 2010-2011 runs by the NSSL runs and 2011 runs by CAPS have been examined and used to make revisions to the LFA for 2012 and subsequent years. Emphasis is on the performance of the LFA in the cold season and in very high-flash rate convective storm events, where preliminary inspection of the 2010-2011 data suggest deficiencies in the original LFA. The purpose of this paper is to summarize the most salient findings from 2010-2011, and to describe the 2012 modifications made to the LFA.

2. DATA AND METHODOLOGY

The LFA is a simple proxy-based diagnostic algorithm that can be applied to any suitable explicit-convection model output containing the basic kinematic, thermal and microphysical fields. The algorithm considers two main proxy variables, the upward graupel flux (GFX) in the mixed phase layer, and the total vertical ice integral (VII), as proxies for total lightning flash rate densities. For GFX, the layer with temperature of -15°C is taken as the mixed phase layer. Both proxies have been found in global observational studies (Petersen et al. 2005; Cecil et al. 2005; Deierling and Peterson 2008) to be strongly related to storm flash rates. In McCaul et al. (2009), the peak values of the two simulated proxies in convective events in the Tennessee Valley area were found to be linearly related to the peak total lightning flash origin densities observed by the North Alabama Lightning Mapping Array (NALMA; Goodman et al. 2005; Krehbiel et al. 2000). Each proxy peak value was paired against the corresponding observed peak flash rate density (FRD) from NALMA, and a linear regression performed to derive a coefficient that could serve to calibrate each proxy against NALMA observations. After this calibration procedure, both proxies produced fields of diagnosed total FRD that had values in the strongest storms that were an approximate match for the peak observed FRD values seen by NALMA.

The GFX-based FRD fields resembled the VII-based fields, but showed more compact spatial footprints and more realistic temporal variability. The smoothness of VII was due to the effect of the integrations used in its computation. Thus, GFX appeared to be properly calibrated but more sensitive to storm updraft variations. VII, while also properly calibrated, had the advantage of better depicting the spread of total lightning channels into storm anvil regions. To achieve a more optimum result, having both a realistic time variability but with larger spatial footprint, McCaul et al. (2009) computed a blended field, based on a weighted average of the GFX and VII fields. Assignment of a weight of 0.95 to GFX and 0.05 to VII was found to preserve most of the desired temporal variability, while producing a net spatial footprint consistent with NALMA observations of the areal coverage of total lightning threat, based on flash extent density (Murphy and Demetriades 2005; Lojou and Cummins 2005).

The LFA was originally designed and calibrated on a 2 km x 2 km grid, using WRF runs performed on a series of diverse convective weather events over the Tennessee Valley region. The microphysics scheme used was the WRF Single Moment-6 species scheme (WSM6), which can be specified to contain graupel, believed to be an essential hydrometeor species in the non-inductive charging process (Mansell et al. 2002;

*Corresponding author address: Eugene W. McCaul, Jr., Universities Space Research Association, 320 Sparkman Drive Huntsville, AL 35805, e-mail: emccaul@usra.edu

Mansell et al. 2005). McCaul et al. (2009) point out that their calibration constants should be reevaluated for models configured with other microphysics schemes or run on other grid meshes.

The daily 36-h NSSL WRF runs in 2010-2011 were performed on a native 4 km x 4 km grid approximately the size of the continental United States (CONUS), using the WSM6 microphysics scheme. The almost-daily 36-h CAPS WRF runs conducted in Spring 2011 were run on a grid comparable in size and resolution, but with considerable diversity in the choice of microphysics and other physics schemes, and in perturbations added to the initial conditions. The LFA was added to both models without modification, to see what sensitivities existed to the changes in model mesh and physics scheme choices. To ensure the actual peak values of LFA-derived FRD were recorded for analysis and comparison with LMA 5-min data, hourly fields of the hourly maximum values of the simulated GFX, VII and blended lightning FRD estimates were saved and examined, as in Kain et al. (2010). Statistics were compiled describing the daily peak values of each of these three FRD threat estimates, both over the CONUS and within smaller mesoscale regions near Huntsville, Alabama (HUN) and Norman, Oklahoma (OUN), where validating LMA data are available. To check the accuracy of the LFA calibrations, scatterplots of the peak values of the GFX-based threat and VII-based threat were constructed, and any noteworthy deviations from the expected diagonal pattern were recorded. For selected weather events of interest, LMA data were obtained and analyzed to produce fields of gridded FRD on the same grid used for inspection of the WRF LFA data. Of particular interest is the question of which LFA threat, GFX or VII, validates better against LMA observations in cases where the GFX and VII values disagree.

For the CAPS ensembles, some 14 WRF runs were equipped with the LFA. For each hour featuring active convection, peak GFX, VII and blended LFA-based FRD threat values were logged for CONUS, HUN and OUN regions. The 14 separate peak values of each threat were then averaged to create a consensus peak value, and their standard deviation was then evaluated. For each active hour, the ensemble mean of the peak FRD threats was then used as the abscissa of a scatterplot, against which the largest and smallest of the 14 ensemble peak values and their standard deviations could be plotted. To study the performance of the LFA in specific WRF configurations, the scatterplots could be embellished with markings depicting the actual peak threat values for that specific model run. This tactic was useful in identifying model configurations for which the LFA tended to overperform or underperform, compared to consensus.

3. RESULTS AND DISCUSSION

Inspection of data from the 2010-2011 NSSL and 2011 CAPS runs have shown that the LFA produces generally reasonable lightning FRD fields, but that it tends to underforecast lightning rates in extreme storms, and to produce numerous false alarms in the winter months. Initial concerns about the effect of 4-km model meshes on the LFA FRD estimates, where updraft speeds were expected to be weaker and GFX values correspondingly smaller than in the original 2 km study, turned out to be relatively unimportant. Of more concern were discrepancies in the peak FRD values from GFX and VII for very high flash-rate storms encountered in the warm season. In particular, a scatterplot of LFA event peak FRDs for the GFX and VII threats reveals that both threats remain approximately equal up to FRD values of about 15 fl km^{-2} $(5\ min)^{-1}$. For very active storms having FRDs in excess of that threshold, VII consistently exhibits smaller peak values relative to GFX (Fig. 1). Validation against available LMA data reveals that GFX values are more accurate than VII at very high FRD. It appears that the VII parameter may suffer from natural moisture-based limits on its maximum values in very moist warm-season regimes, while GFX, mainly dependent on midlevel updraft speed, suffers much less from such limitations.

By contrast, the presence of ice in cold stratiform cloud systems, especially in seasons other than summer, tends to trigger LFA false alarms, such that the VII FRD threat values in such cases are often biased high. Such false alarms are most common in very low flash rate situations. We also see evidence that WRF tends to overpredict convective storms during the warm season; of all warm season days examined in 2010-2011 NSSL runs, WRF showed deep convection on 181 days, whereas actual deep convection occurred on only 169 days.

These anomalous behaviors of the LFA were relatively easy to remedy. Several simple changes to the LFA were implemented for use in 2012 forward. To improve LFA FRD estimates in high flash rate storms, we now require that the VII proxy have its peak value forcibly set equal to that from the GFX proxy before the blending step. In general, we have found it desirable to rely mainly on GFX in both high and low flash rate regimes. In addition, we now mandate a higher GFX threshold of 1.5 fl km^{-2} $(5\ min)^{-1}$ for screening out spurious weak lightning threats. Based on the data from 2010-2011, the use of this higher threshold for GFX has the effect of eliminating approximately 85% of the winter season false alarms, without compromising the performance of the algorithm in the warm season. A rare, genuine thundersnow event documented in the NALMA region on 10 January 2011 would not have been eliminated by this new choice of minimum threat threshold. Most of the 15% of remaining winter false alarms appear to be WRF forecasts of sleet, most of which were localized erroneous forecasts of precipitation type.

Analyses of LFA results from the 2011 CAPS WRF ensemble members reveal that most combinations of physics packages employed yielded lightning flash rate estimates somewhat smaller than that from the default WSM6 configuration used for LFA development (Fig. 2), and that there is a not unexpected sensitivity to variations in the microphysics and other physics schemes used. This sensitivity tends to increase slowly with the amounts of lightning forecast, such that the absolute variability is largest for very high lightning events, but the relative or fractional variability is largest for very low lightning events. Given the systematic low bias of LFA results from CAPS members equipped with the Thompson 2-moment microphysics scheme (Fig. 3), which is also used in the operational HRRR model, we plan to study in more detail the performance of the LFA in the HRRR, and to perform a custom recalibration of the LFA for that model.

4. ACKNOWLEDGMENTS

This research was funded by a Risk Reduction grant from the National Oceanic and Atmospheric Administration to Project 68, in support of the planned launch of the Geostationary Lightning Mapper (GLM) on the GOES-R satellite platform.

5. REFERENCES

Cecil, D. J., S. J. Goodman, D. J. Boccippio, E. J. Zipser, and S. W. Nesbitt, 2005: Three years of TRMM precipitation features. Part I: Radar, radiometric, and lightning characteristics. *Mon. Wea. Rev.*, **133**, 543–566.

Deierling, W., and W. A. Petersen, 2008: Total lightning activity as an indicator of updraft characteristics. *J. Geophys. Res.*, *113*, D16210, doi: 10.1029/2007JD009598.

Goodman, S. J., R. Blakeslee, H. Christian, W. Koshak, J. Bailey, J. Hall, E. McCaul, D. Buechler, C. Darden, J. Burks, T. Bradshaw, and P. Gatlin, 2005: The North Alabama Lightning Mapping Array: Recent severe storm observations and future prospects. *Atmos. Res.*, **76**, 423–437.

Kain, J. S., S. R. Dembek, S. J. Weiss, J. L. Case, J. J. Levitt, and R. A. Sobash, 2010: Extracting unique information from high-resolution forecast models: Monitoring selected fields and phenomena every time step. *Wea. Forecasting*, **25**, 1536–1542.

Krehbiel, P.R., R.J. Thomas, W. Rison, T. Hamlin, J. Harlin, and M. Davis, 2000: GPS-based mapping system reveals lightning inside storms. *Eos*, **81**, 21–25.

Lojou, J.-Y., and K. L. Cummins, 2005: On the representation of two- and three-dimensional total lightning information. *Preprints CD-ROM*, 1st Conf. Meteorol. Appl. Lightning Data, San Diego, CA, Amer. Meteor. Soc., paper 2.4.

Mansell, E. R, D. R. MacGorman, C. L. Ziegler, and J. M. Straka, 2002: Simulated three-dimensional branched lightning in a numerical thunderstorm model. *J. Geophys. Res.*, *107*, 4075, doi: 10.1029/2000JD000244.

Mansell, E. R, D. R. MacGorman, C. L. Ziegler, and J. M. Straka, 2005: Charge structure and lightning sensitivity in a simulated multicell thunderstorm. *J. Geophys. Res.*, *110*, D12101, doi: 10.1029/2004JD005287.

McCaul, E. W., Jr., S. J. Goodman, K. M. LaCasse, and D. J. Cecil, 2009: Forecasting lightning threat using cloud-resolving model simulations. *Wea. Forecasting*, **24**, 709–729. (highlighted as a Paper of Note in *Bull. Amer. Meteorol. Soc.*, **90**, 772.)

Murphy, M. J., and N. Demetriades, 2005: An analysis of lightning holes in a DFW supercell storm using total lightning and radar information. *Preprints CD-ROM*, 1st Conf. Meteorol. Appl. Lightning Data, San Diego, CA, Amer. Meteor. Soc., paper 2.3.

Petersen, W. A., H. J. Christian, and S. A. Rutledge, 2005: TRMM observations of the global relationship between ice water content and lightning. *Geophys. Res. Lett.*, 26 July 2005, **32;14**, L14819 doi: 10.1029/2005GL023236.

Skamarock, W. C., J. B. Klemp, J. Dudhia, D. O. Gill, D. M. Barker, M. G. Duda, X.-Y. Huang, W. Wang, and J. G. Powers, 2008: A description of the Advanced Research WRF Version 3. NCAR Technical Note NCAR/TN-475+STR, 123 pp. [available online at: http://www.mmm.ucar.edu/wrf/users/docs/arw_v3.pdf]

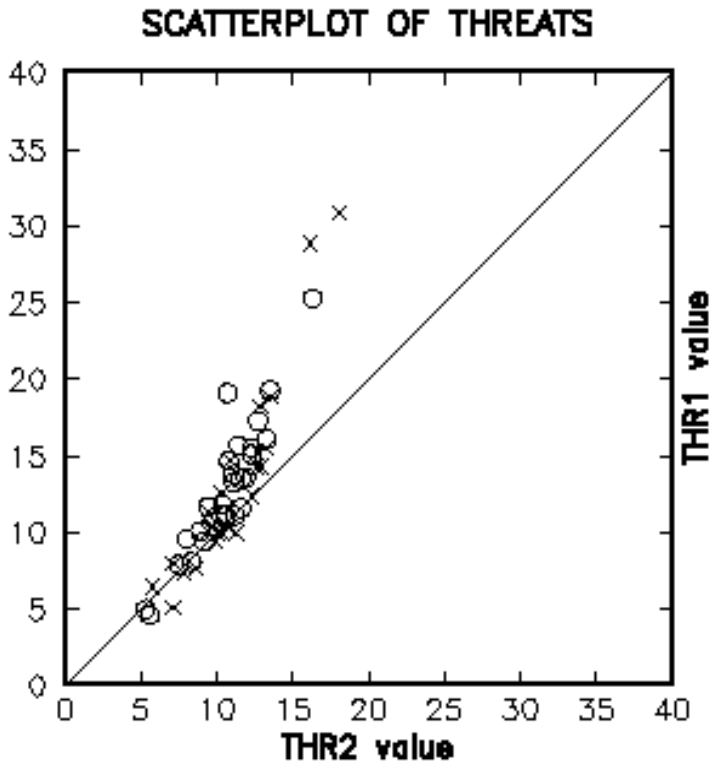

Fig. 1. Scatterplot of values of graupel flux lightning threat (THR1) as a function of vertical ice integral threat (THR2). Data derived from selected NSSL daily WRF runs in 2010-2011, and units are fl km^{-2} (5 $min)^{-1}$. Note deviations off diagonal for larger lightning threat values, with vertical ice integral values consistently too small relative to graupel flux values.

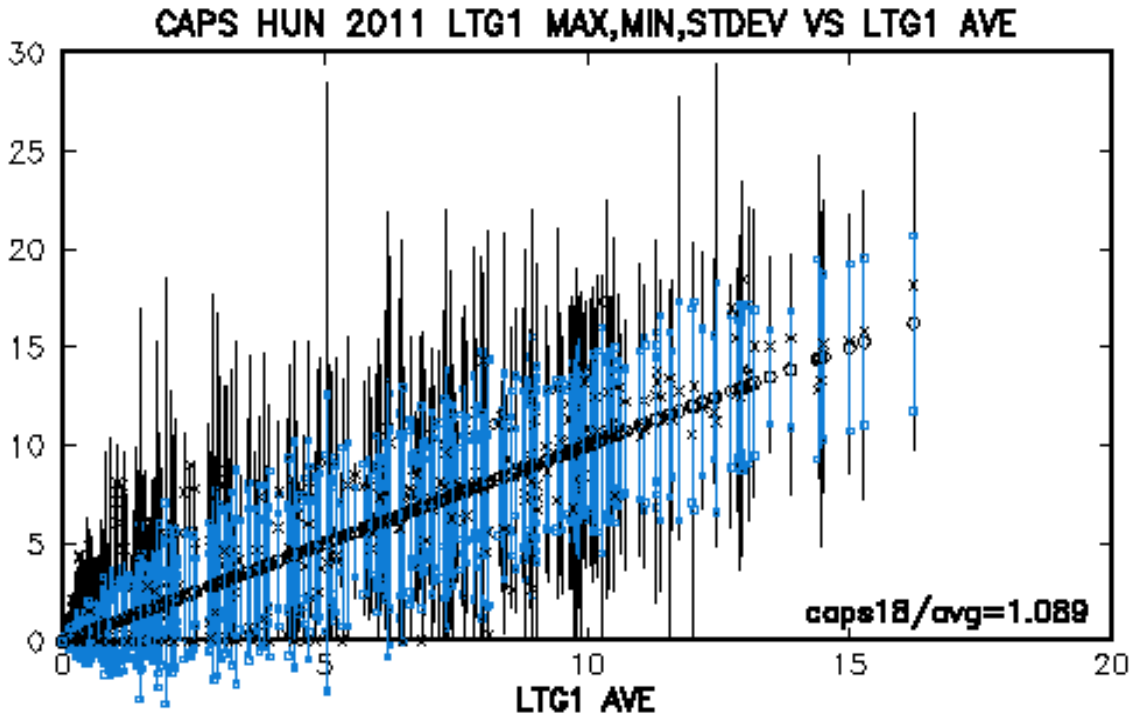

Fig. 2. Scatterplot of values of graupel flux lightning threat (LTG1) maximum, minimum, mean (along diagonal) and standard deviation (bold blue vertical bars), as a function of ensemble mean graupel flux lightning threat, for all convectively active hours of the CAPS runs from the 2011 Spring Experimental Forecast Program of the Hazardous Weather Testbed. Units are fl km^{-2} $(5\ min)^{-1}$. Small "x" symbols depict actual data from only the WSM-6 microphysics runs, which exceed the ensemble means by a factor of 1.089.

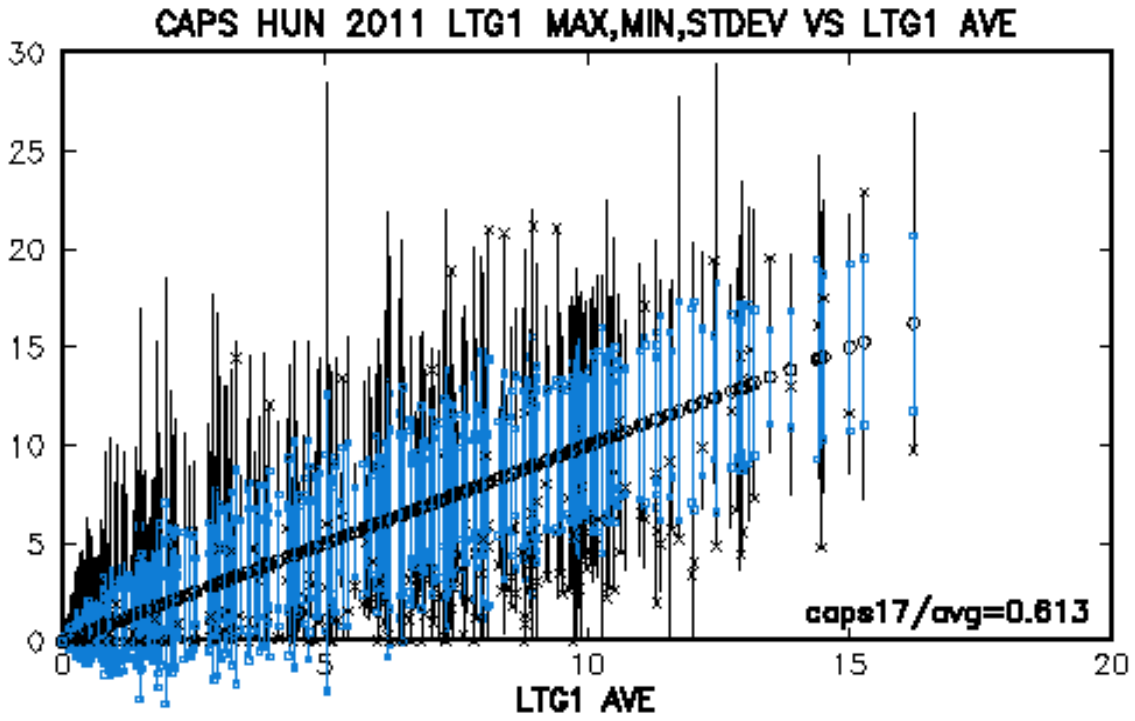

Fig. 3. Scatterplot as in Fig. 2, but with small "x" symbols depicting actual data from only the Thompson double-moment microphysics runs, which fall short of the ensemble means by a factor of 0.613.